ORIGINAL ARTICLE

Comparison of tumor related signaling pathways with known compounds to determine potential agents for lung adenocarcinoma

Song Xu[1,2], Renwang Liu[1,2] & Yurong Da[3]

1 Department of Lung Cancer Surgery, Lung Cancer Institute, Tianjin Medical University General Hospital, Tianjin, China
2 Tianjin Key Laboratory of Lung Cancer Metastasis and Tumor Microenvironment, Lung Cancer Institute, Tianjin Medical University General Hospital, Tianjin, China
3 Key Laboratory of Cellular and Molecular Immunology in Tianjin, Key Laboratory of Immune Microenvironment and Disease of the Ministry of Education, Department of Immunology, School of Basic Medical Sciences, Tianjin Medical University, Tianjin, China

Abstract

Background: This study compared tumor-related signaling pathways with known compounds to determine potential agents for lung adenocarcinoma (LUAD) treatment.

Methods: Kyoto Encyclopedia of Genes and Genomes signaling pathway analyses were performed based on LUAD differentially expressed genes from The Cancer Genome Atlas (TCGA) project and genotype-tissue expression controls. These results were compared to various known compounds using the Connectivity Mapping dataset. The clinical significance of the hub genes identified by overlapping pathway enrichment analysis was further investigated using data mining from multiple sources. A drug-pathway network for LUAD was constructed, and molecular docking was carried out.

Results: After the integration of 57 LUAD-related pathways and 35 pathways affected by small molecules, five overlapping pathways were revealed. Among these five pathways, the p53 signaling pathway was the most significant, with *CCNB1*, *CCNB2*, *CDK1*, *CDKN2A*, and *CHEK1* being identified as hub genes. The p53 signaling pathway is implicated as a risk factor for LUAD tumorigenesis and survival. A total of 88 molecules significantly inhibiting the five LUAD-related oncogenic pathways were involved in the LUAD drug-pathway network. Daunorubicin, mycophenolic acid, and pyrvinium could potentially target the hub gene *CHEK1* directly.

Conclusion: Our study highlights the critical pathways that should be targeted in the search for potential LUAD treatments, most importantly, the p53 signaling pathway. Some compounds, such as ciclopirox and AG-028671, may have potential roles for LUAD treatment but require further experimental verification.

Introduction

Lung adenocarcinoma (LUAD) is a subtype of non-small cell lung cancer (NSCLC). It is the most common type of lung cancer in the world, with particularly poor prognosis in patients who have reached advanced stages.[1–5] Because of the low diagnosis rates in the early stages of the disease, most patients are diagnosed with LUAD when it is too late to effectively treat with surgical removal (approximately 70% in China). With the development of tumor-targeted drugs, some LUAD patients may receive a curative effect. EGFR-tyrosine kinase inhibitors (TKIs) have become an indispensable therapeutic strategy in advanced NSCLC patients with *EGFR* sensitive mutations, such as those in exons 19 and 21. Nevertheless, drug resistance frequently occurs during therapy, minimizing the ability to control disease progression.[6–14] Urgent investigation of the pathways

related to the mechanisms of drug resistance is being conducted to determine the critical biological agents of this process. Differentially expressed genes (DEGs) in lung cancer and non-cancerous lung tissues can be used to identify novel signaling pathways and reliable biomarkers that may lead to therapeutic targets.

The Cancer Genome Atlas (TCGA; http://cancergenome. nih.gov/) is a collaborative database that features comprehensive, multi-dimensional maps of the key genomic changes in cancer. The database contains both tumor tissues and matched normal tissues from a large number of patients and has been widely used in the research community.[15–20] The Connectivity Map (CMap; http://www.broadinstitute.org/cmap/) is a resource that uses transcriptional expression data to probe relationships between diseases, cell physiology, and therapeutics. CMap seeks to uncover novel treatments for a variety of diseases, including cancers, and neurological and infectious diseases.[21–25]

The combination of the enrichment inquiry of crucial cancer-related genes from TCGA and the CMap analysis indicates that signaling genes may be prospective drug targets for therapy in certain tumors[26] such as ovarian cancer[21,27] and hepatocellular carcinoma.[25] In the current study, we performed an in silico investigation using CMap analysis of the DEGs gathered from a large population of LUAD patients ($n = 483$). This process led to the identification of prospective candidate drugs for future LUAD treatments.

Methods

Lung adenocarcinoma (LUAD) signaling pathways

TCGA provided 19 123 messenger RNA (mRNA) expression levels from 483 LUAD cases by RNA-sequencing. For comparison, 347 cases of matched normal and genotype-tissue expression controls were provided by the Gene Expression Profiling Interactive Analysis platform from the University of California Santa Cruz Xena Project (http://xena.ucsc.edu).[18,28–31] All expression data were transformed into Log 2 (transcripts per kilobase million [TPM] + 1) for further calculation. The fold change of the mRNA expression levels was calculated using the difference between the LUAD samples and the non-cancerous controls. The cutoffs to classify an mRNA as being abnormally expressed were Log 2 fold change > 1 and a q-value < 0.05. Analysis of variance was utilized for the differential expression analysis. The DEGs identified from the LUAD tissues were subjected to Kyoto Encyclopedia of Genes and Genomes (KEGG) signaling pathway analysis with the Database for Annotation, Visualization and Integrated Discovery

(DAVID). A false discovery rate of < 0.1 was regarded as statistically significant for the KEGG pathway analysis.[32–35]

Signaling pathways of known compounds from the Connectivity Map (CMap)

CMap provides a data resource to interpret a drug's prospective molecular mechanisms using genome-wide gene signatures. Over 7000 expression profiles corresponding to 1309 compounds are publicly available from the online CMap database (build02). The microarray data for each of the compounds was downloaded and the DEGs were calculated by comparing treatment and control groups.[21–25] A fold change of > 2 or < 0.5 was used to identify the DEGs, which were subsequently subjected to KEGG pathway analysis using the procedure followed in a previous report.[25]

Potential novel drugs for LUAD

The significant pathways involved in the onset of LUAD and those affected by the CMap drugs were integrated. The compounds involved in these overlapping pathways were considered to be potential drugs for the treatment of LUAD. Rank-based pattern-matching processes were employed to perform a similarity evaluation of various pharmaceutical substances. The statistical significance was computed based on random permutations. The top 10 compounds are listed in Figure S1 along with their molecular structures, as provided by PubChem Compound (https://www.ncbi.nlm.nih.gov/pccompound).

Gene ontology analysis and protein–protein interaction of the genes in the overlapping pathways

To reveal the overall function of genes enriched in the overlapping pathways, gene ontology analysis was performed by DAVID and the results were displayed in a gene ontology plot using R software ggplot2 packages (R Foundation for Statistical Computing, Vienna, Austria). Protein–protein interaction was conducted to draw the gene network.[36–39]

Construction of the drug-pathway network

Because the five overlapping pathways may be important for targeting novel molecules, a drug-pathway network was constructed. Molecules corresponding to these five pathways were collected and entered into Cytoscape software (National Institute of General Medical Sciences, Bethesda, MD, USA). Lines between the pathways and molecules

represent a potential relationship between the drugs and the corresponding pathways.

Clinical significance of hub genes enriched in the p53 signaling pathway

The p53 signaling pathway was the most significant pathway related to the effect of known compounds. The expression patterns and prognostic values of the hub genes from the p53 signaling pathway were comprehensively analyzed. The mRNA expression levels of these genes were obtained from the Gene Expression Profiling Interactive Analysis online database. Kaplan–Meier survival plots were used to assess the prognostic roles of these genes.[18,28–31] The corresponding protein expression levels were collected from the Human Protein Atlas to validate the different expression trends between LUAD and non-tumor lung tissues.[40–46] As multiple targets provide a more powerful prognostic value and estimate of treatment potential, several hub genes were pooled as a group and their prognostic implications were assessed based on LUAD TCGA data (*n* = 475), as calculated by the SurvExpress database (47, http://bioinformatica.mty.itesm.mx:8080/Biomatec/SurvivaX.jsp). All probe sets and records were averaged per sample. A prognostic index (PI) of these hub genes was calculated by

Cox survival analysis and the corresponding hazard ratio was analyzed.[47–53]

Predicted binding affinities between hub genes and compounds using molecular docking

To obtain detailed information on how these novel drugs exert anti-tumor functions, molecular docking between the compounds and the proteins of the hub genes enriched in the most significant pathway (the p53 signaling pathway) was carried out using the Surflex-Dock program in Sybyl X-2.0 (Tripos Inc., St Louis, MO, USA). Docking scores were calculated to represent binding affinities.[54–56]

Results

Identification of LUAD signaling pathways

Altogether, 1993 DEGs were gathered from 483 LUAD patients, including 514 upregulated and 1479 downregulated genes (Fig S2). KEGG analysis showed that 57 pathways were significantly related to LUAD. Unsurprisingly, several among these were well-studied pathways involved in the initiation and progression of LUAD: focal adhesion;
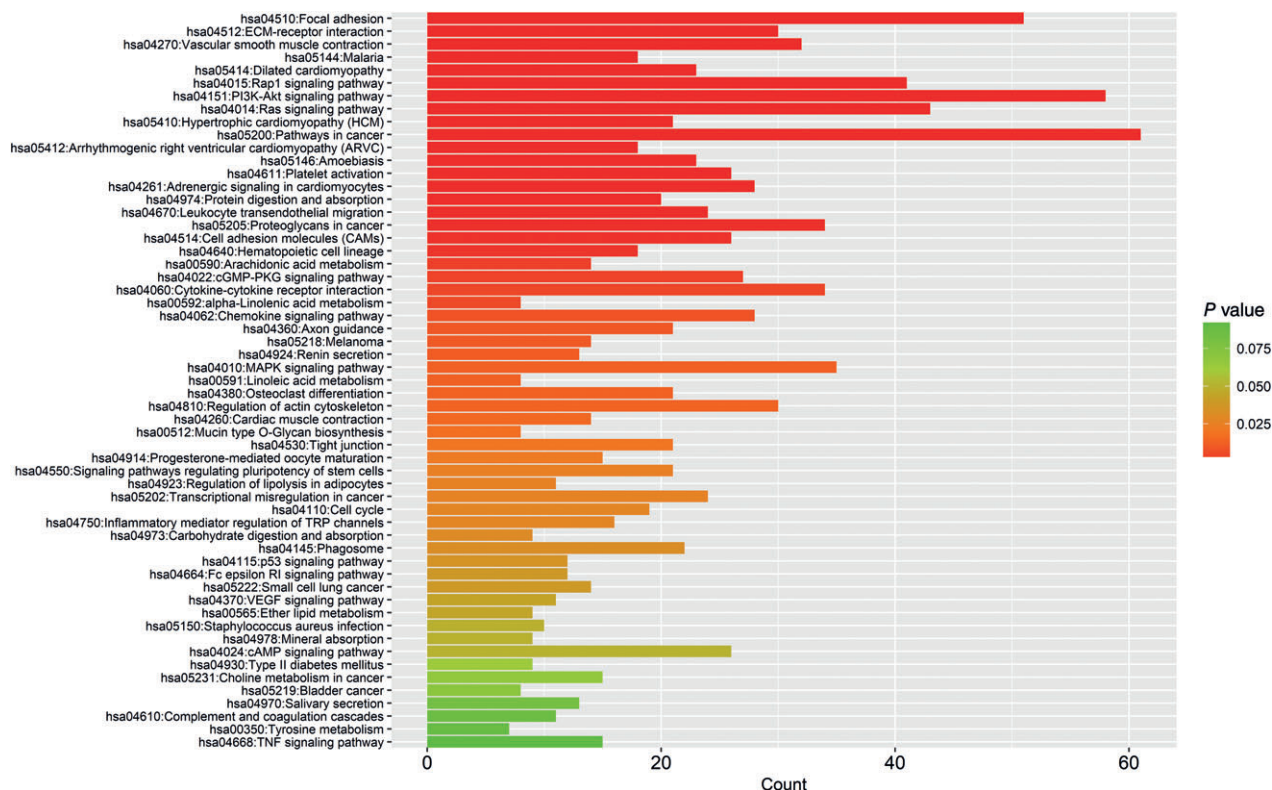

Figure 1 Kyoto Encyclopedia of Genes and Genomes (KEGG) pathway of differentially expressed genes. The length of the bar represents the weight of the number of genes in the pathway. The color represents the significance of the enriched pathways.

extracellular matrix-receptor interaction; Rap1, PI3K-Akt, Ras, chemokine, MAPK, p53, and VEGF signaling pathways; pathways in cancer; proteoglycans in cancer; cell adhesion molecules, and cell cycle (Fig 1; Table S1). Drugs that target these pathways may have the potential to treat LUAD, thus potential candidate molecules were identified.

Pathways affected by known molecular agents in CMap

The global associations between 1309 bioactive small molecular agents and the identified pathways were obtained from the CMap database. Altogether, 35 enriched KEGG pathways were obtained with a false discovery rate of < 0.1. The top 10 significant pathways are displayed in Figure 2a. After the integration of the 57 LUAD-related pathways and the 35 pathways affected by the small molecules, five overlapping pathways were identified that could be targeted by known small molecules (Fig 2b), including pathways in cancer and chemokine, MAPK, p53, and Fc epsilon RI signaling pathways. The p53 signaling pathway was the pathway affected by the most molecules. A total of 44 (44/82) molecules are characterized as having an anti-tumor function that targets the p53 signaling pathway.

Gene ontology and protein–protein interaction analyses

Because these five pathways play essential roles in LUAD tumorigenesis and are likely vital for the discovery of novel drugs, genes enriched in the five pathways were collected and gene ontology analysis was performed to reveal their characteristics and possible molecular mechanisms. The genes characterized as being involved in biological processes were most associated with cell chemotaxis, extracellular matrix organization, and the chemokine signaling pathway (Fig 3a). The genes characterized as being related to cellular components were most associated with the extracellular region, the extracellular space, and the plasma membrane (Fig 3b). As for molecular function, these genes were markedly involved in chemokine, PIK3CA, and Ras guanyl-nucleotide exchange factor activity (Fig 3c). A protein–protein interaction network consisting of the genes in the five pathways was constructed, which revealed a short list of genes that were closely related to each other, including *IL6*, *GNG11*, *FGF2*, *PIK3R1*, and *MMP9* (Fig 4).

Construction of the drug-pathway network

Based on the five common pathways involved in the onset of LUAD and the effect of the unknown molecular drugs, a drug-pathway interaction network was constructed. A total
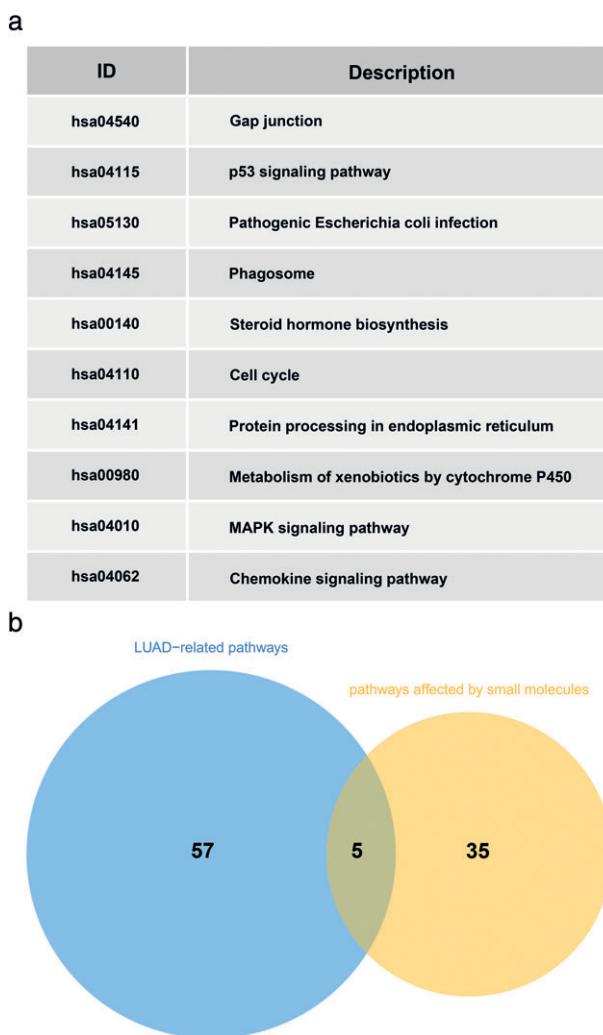
ID	Description
hsa04540	Gap junction
hsa04115	p53 signaling pathway
hsa05130	Pathogenic Escherichia coli infection
hsa04145	Phagosome
hsa00140	Steroid hormone biosynthesis
hsa04110	Cell cycle
hsa04141	Protein processing in endoplasmic reticulum
hsa00980	Metabolism of xenobiotics by cytochrome P450
hsa04010	MAPK signaling pathway
hsa04062	Chemokine signaling pathway

Figure 2 Discovery of potential targeted pathways by Connectivity Map (CMap). (**a**) The enriched pathways that were obtained from CMap. (**b**) Integration of the 57 lung adenocarcinoma (LUAD)-related pathways and the small molecules that affected these pathways.

of 88 molecules significantly inhibiting the five important LUAD-related oncogenic pathways were involved in the drug-pathway network. These compounds may have potential as future anti-LUAD drugs (Fig S3). To reveal the interacting effects of the genes involved in each pathway, a protein–protein interaction link was again constructed for each pathway (Fig S4).

Candidates for novel effective drugs to treat LUAD

The relationships between the five pathways and the novel molecules were analyzed. The top 10 significant drugs all
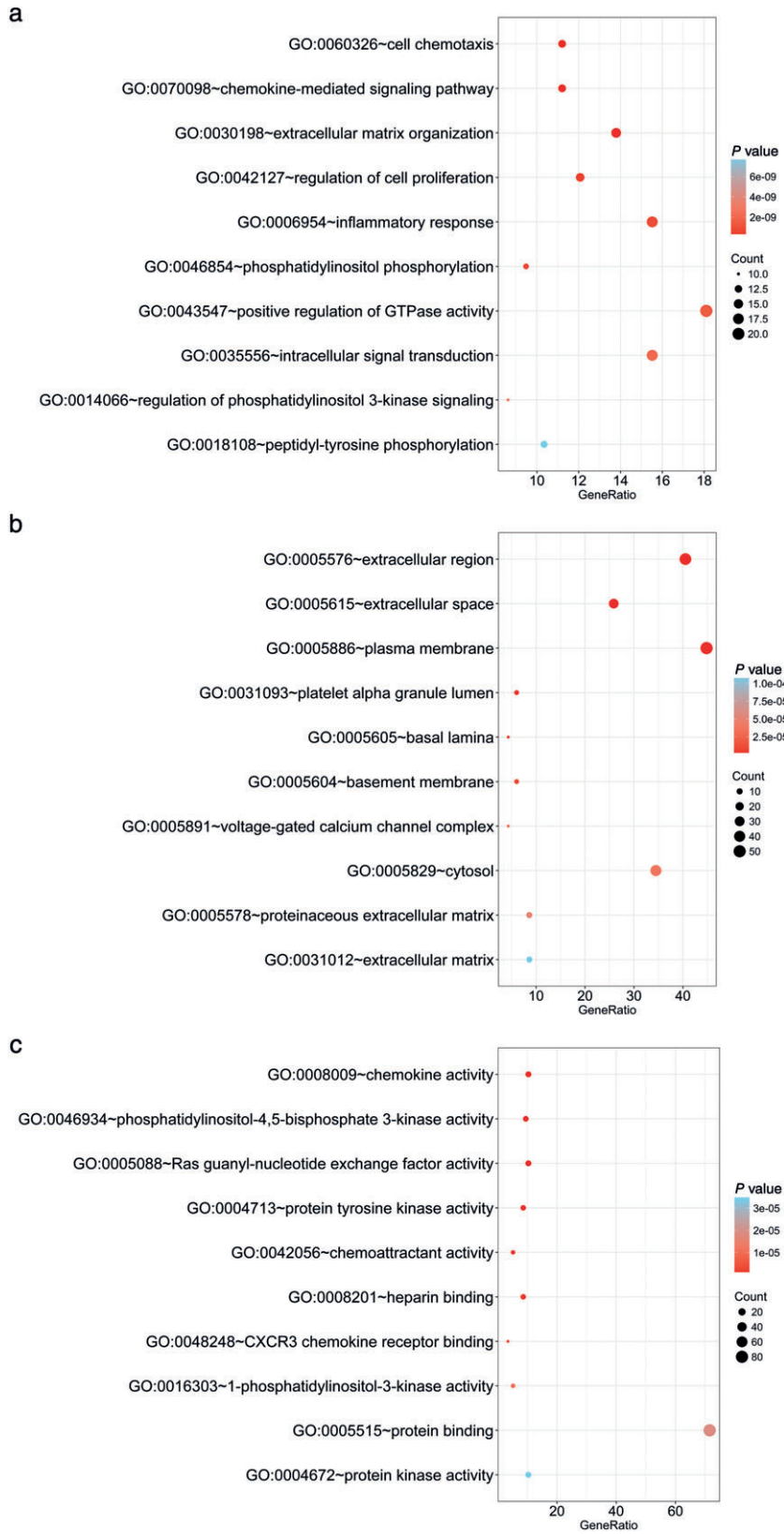
Figure 3 Gene ontology of genes enriched in the five overlapping pathways. (**a**) Biological process; (**b**) cellular component; and (**c**) molecular function.
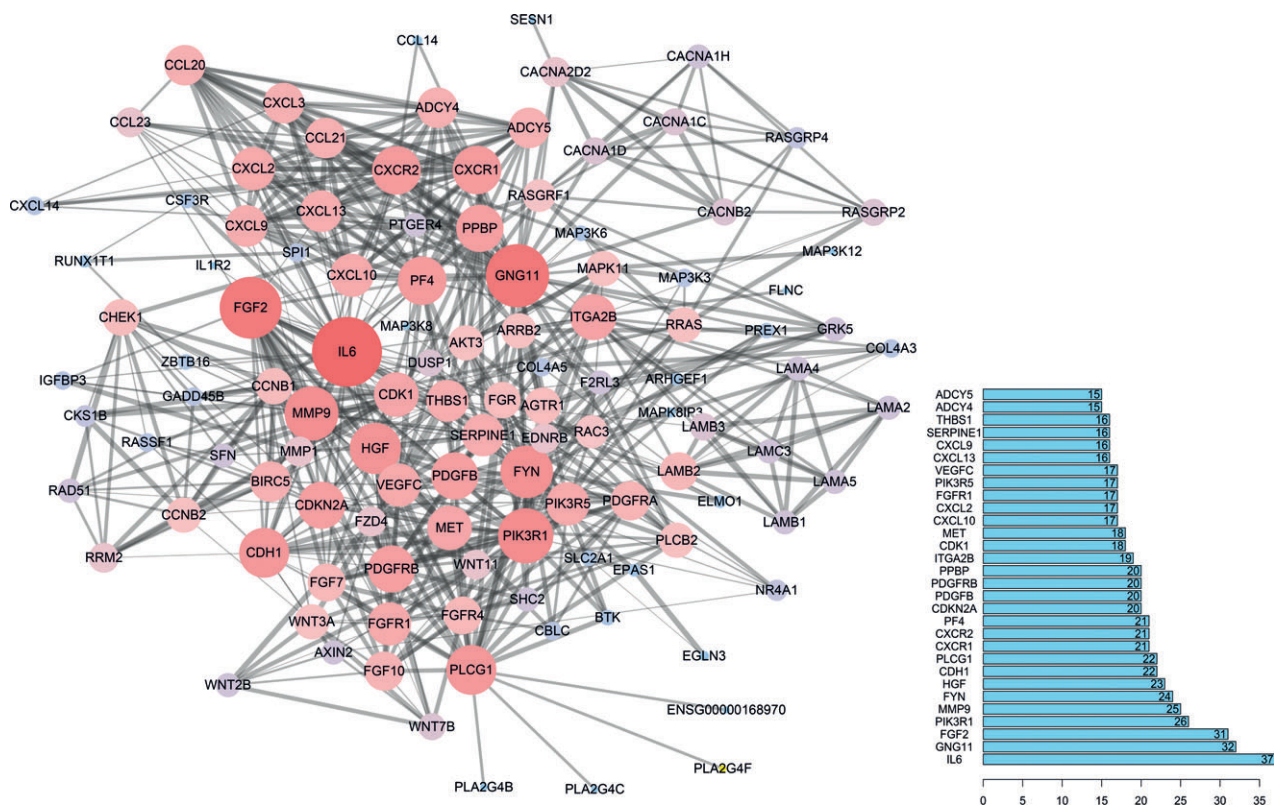
Figure 4 Protein–protein interactions of genes enriched in the five overlapping pathways. The size of the circle represents the weight of the gene in the network. The thickness of the line reflects the connection score between two genes.

interacted with the p53 signaling pathway (Fig 5): etoposide, irinotecan, camptothecin, pyrvinium, metyrapone, trifluridine, mycophenolic acid, resveratrol, AG-028671, and daunorubicin (Fig S4).

Clinical significance of the p53 signaling pathway in LUAD

The five hub genes of the p53 signaling pathway are *CCNB1*, *CCNB2*, *CDK1*, *CDKN2A*, and *CHEK1*. As expected, the mRNA expression levels of these genes were markedly upregulated in LUAD tissues compared to normal lung tissues (Fig S5). Protein expression levels also showed a consistent trend (Fig 6). Significantly, overexpression of these genes is associated with lower survival rates in LUAD patients (Fig 7). Consequently, a PI model was generated to predict a patient's overall chance of survival in combination with the upregulation of these five genes (Fig 8), using the formula: PI = (0.378* expression level of *CCNB1*) + (−0.781* expression level of *CCNB1*) + (0.704* expression level of *CDK1*) + (0.012* expression level of *CDKN2A*) + (0.315* expression level of *CHEK1*). Patients were divided into high and low-risk groups based on the PI model, and the five genes were all upregulated in the high-risk group (Fig 9a). Multivariate analysis

demonstrated a hazard risk of 1.55 (95% confidence interval 1.14–2.11; P = 0.005), indicating that the p53 signaling pathway is a risk factor in the survival outcome of LUAD patients (Fig 9b).

Correlations between hub genes and compounds identified using molecular docking

To examine if the potential effects of the molecules involved in the p53 signaling pathway were related to direct targeting between compounds and genes, molecular docking analysis was performed. The hub gene from the p53 signaling pathway that revealed the greatest clinical significance was *CHEK1*. Little research regarding the role of *CHEK1* in LUAD has been reported, thus *CHEK1* was selected for molecular docking analysis. Intriguingly, the top 10 molecules all exerted moderate binding capacity to *CHEK1* (Table S2). Daunorubicin, mycophenolic acid, and pyrvinium exhibited the highest connection scores (Fig 10).

Discussion

In the current study, we speculated that prospective compounds for LUAD treatment and therapy are involved in
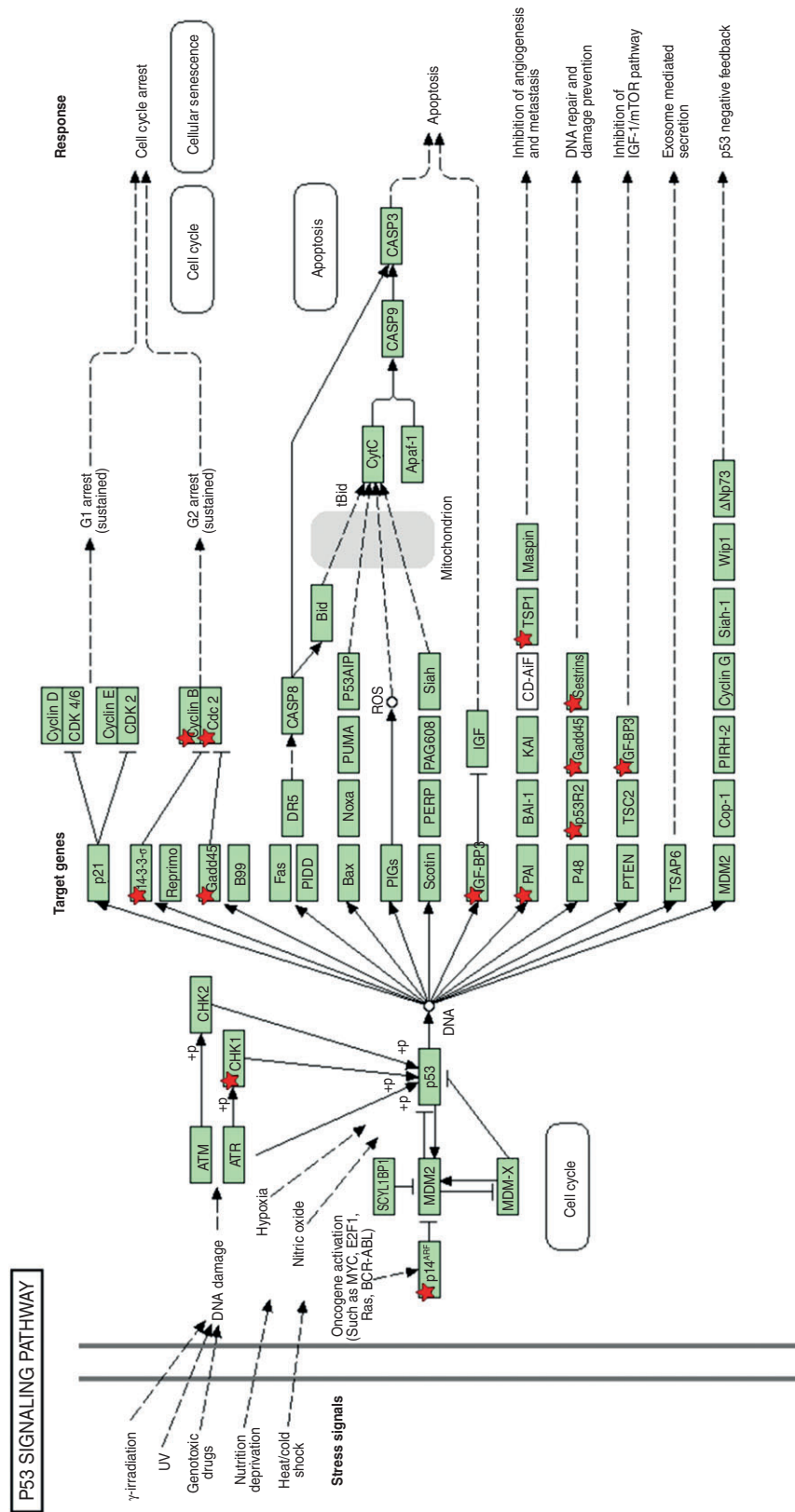
Figure 5 p53 signaling pathway. The red star indicates differentially expressed genes of lung adenocarcinoma enriched in the p53 signaling pathway.
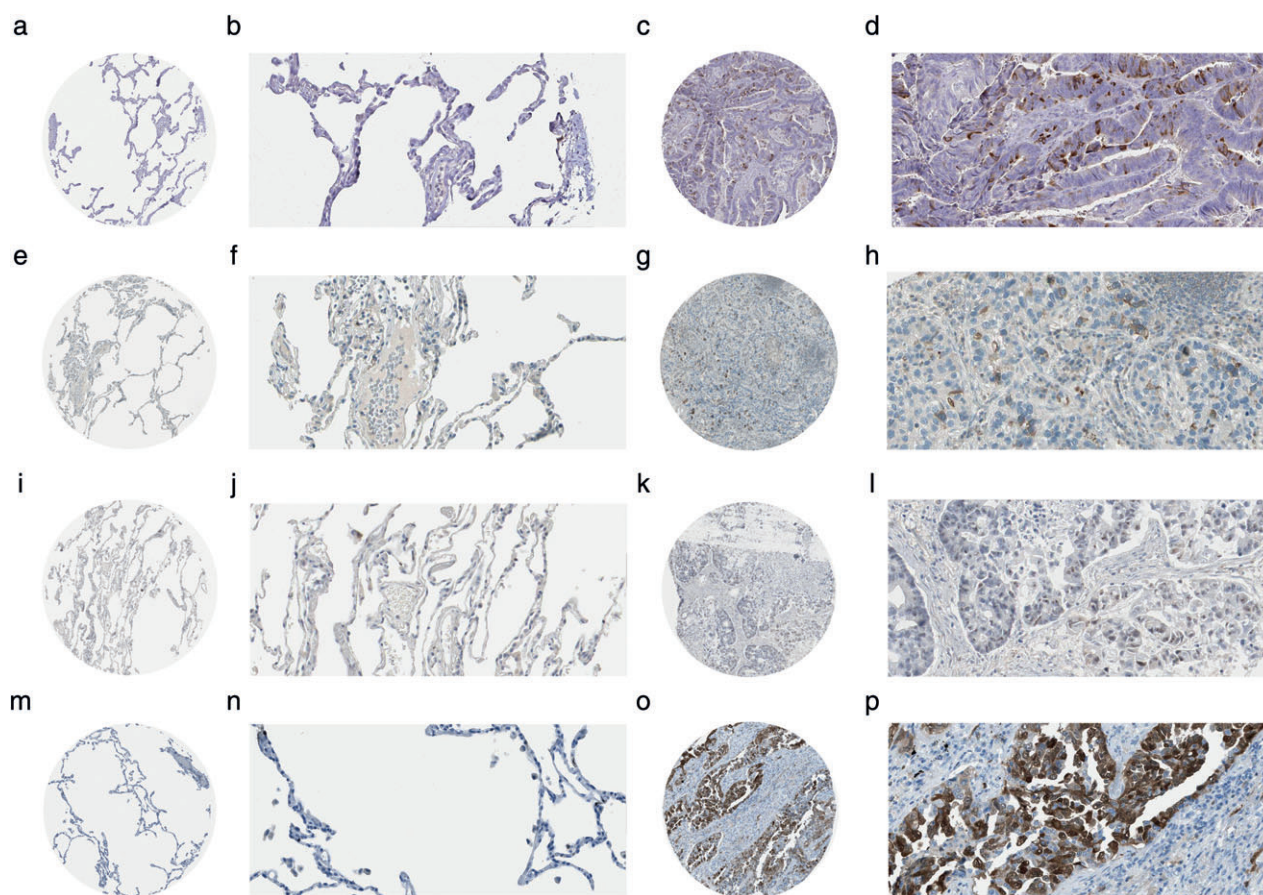
Figure 6 The protein expression level of four hub genes in the p53 signaling pathway stained by immunohistochemistry. *CCNB1* expression is significantly higher in (**c,d**) lung adenocarcinoma (LUAD) than (**a,b**) non-tumor tissues. *CCNB2* expression is significantly higher in (**g,h**) LUAD than (**e,f**) non-tumor tissues. *CDK1* expression is significantly higher in (**k,l**) LUAD than (**i,j**) non-tumor tissues. *CCNB2* expression is significantly higher in (**o,p**) LUAD than (**m,n**) non-tumor tissues. Magnification: ×100 (**a,c,e,g,i,k,m,o**) or ×400 (**b,d,f,h,j,l,n,p**).

the signaling pathways related to LUAD tumorigenesis. LUAD DEGs were identified in TCGA and subjected to KEGG signaling pathway analysis. The identified pathways were overlapped with those available from CMap, resulting in five significant common pathways. Among these five pathways, the p53 signaling pathway consisting of 13 genes was related to the most molecules from the CMap dataset. Based on multiple data mining, five hub genes from the p53 signaling pathway (*CCNB1*, *CCNB2*, *CDK1*, *CDKN2A*, and *CHEK1*) were found to play an essential role in the occurrence and development of LUAD. Molecule docking techniques revealed that daunorubicin, mycophenolic acid, and pyrvinium could bind directly to *CHEK1*. In addition, several known compounds that have never been associated with LUAD, including AG-028671 and ciclopirox, were identified as being worthy of further investigation for the treatment of LUAD.

It is interesting to discover that five classical signaling pathways play pivotal roles in the tumorigenesis of LUAD and can be targeted by known compounds. These five pathways, including pathways in cancer, and chemokine, MAPK, p53, and Fc epsilon RI signaling pathways, have been studied in multiple cancers, including LUAD.[57–68] After analyzing these five pathways in CMap, several known compounds were identified. Unsurprisingly, many among the top 10 have been studied for the treatment of LUAD, including etoposide,[69–71] irinotecan,[72–76] resveratrol,[77–79] and daunorubicin.[80–82] This finding confirms that several well-known anti-cancer drugs used in LUAD treatment fulfill their function by targeting the five aforementioned signaling pathways. This also demonstrates the feasibility of the current methods of combining pathways identified by DEGs and CMap.

Little is known of the relationship of four of the compounds identified in this analysis to LUAD: pyrvinium,[83] metyrapone,[84] trifluridine,[85,86] and mycophenolic acid.[87,88] These compounds have the potential to be used in future LUAD treatments, as they can inhibit vital LUAD pathways. Most importantly, two of these known compounds,
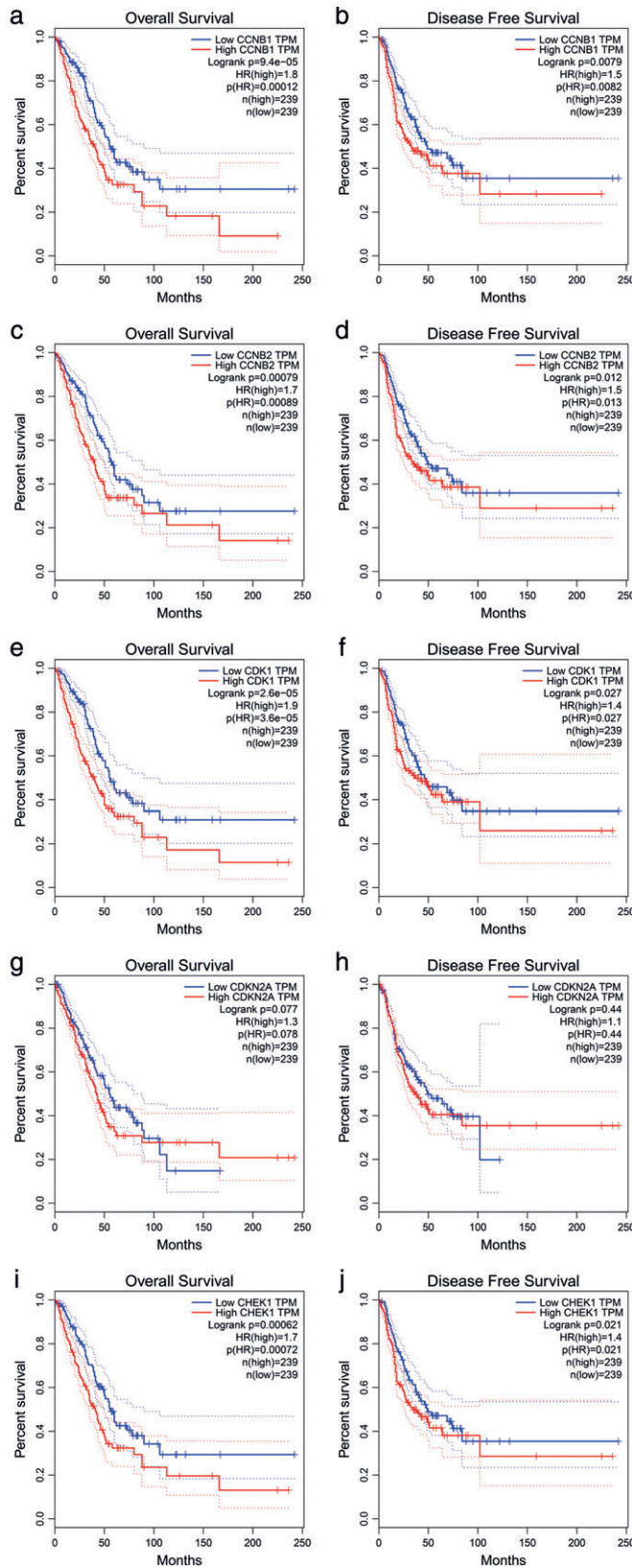
Figure 7 Kaplan–Meier analysis revealed the prognostic value of the five hub genes. Prognostic value of *CCNB1* for predicting (**a**) overall survival (OS) and (**b**) disease-free survival (DFS) of lung adenocarcinoma (LUAD) patients. Prognostic value of *CCNB2* for predicting (**c**) OS and (**d**) DFS of LUAD patients. Prognostic value of *CDK1* for predicting (**e**) OS and (**f**) DFS of LUAD patients. Prognostic value of *CDKN2A* for predicting (**g**) OS and (**h**) DFS of LUAD patients. Prognostic value of *CHEK1* for predicting (**i**) OS and (**j**) DFS of LUAD patients.
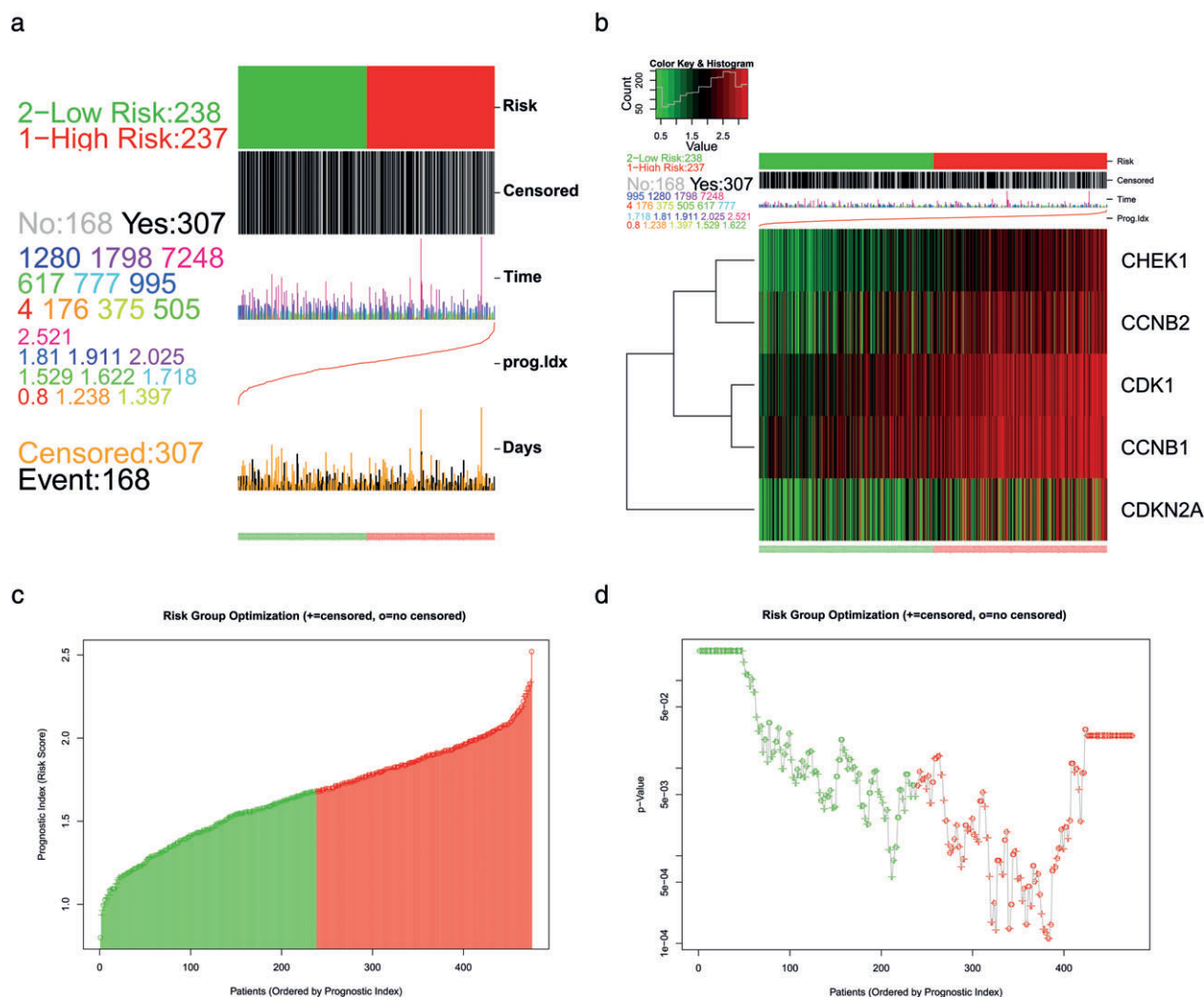
Figure 8 Construction of prognosis index (PI). (**a**) Available clinical information related to risk group, PI, and clinical outcome. (**b**) A heatmap representation of the gene expression values. (**c**) The low and high score groups for the PI in lung adenocarcinoma patients. (**d**) A box plot across risk groups ordered by PI.

ciclopirox and AG-028671, have never been evaluated in LUAD. Ciclopirox is a protein synthesis inhibitor that decreases DNA and RNA replication and protein synthesis, and has been studied as a potential treatment for other cancers.[89–91] However, no information could be obtained for AG-028671, which may be a new drug for the treatment of LUAD. These in silico findings should be confirmed with further experiments.

Because the p53 signaling pathway was the most significant pathway in the CMap analysis and the top 10 compounds were all enriched in this pathway, we examined the clinical role of this pathway using different levels of data mining, including mRNA and protein. The five hub genes (*CCNB1*, *CCNB2*, *CDK1*, *CDKN2A*, and *CHEK1*) were all profoundly upregulated in the LUAD tissues. Moreover, all

of the hub genes are risk factors for LUAD survival. When these five genes were placed into a risk pool, the PI verified them to be an independent factor to predict the overall survival of LUAD patients, confirming that the p53 signaling pathway has a critical function in the progression of the disease. These results verify the significance of the novel drugs that have been discovered. Using molecular docking, we found that the top 10 molecules can significantly affect the hub genes, some by targeting *CHEK1* directly, especially daunorubicin, mycophenolic acid, and pyrvinium. As the genes involved in the overlapping pathways play substantial roles in the development of LUAD, the interference of these genes by powerful drugs can suppress their function. However, future in vivo or in vitro experiments are required to confirm whether these drugs
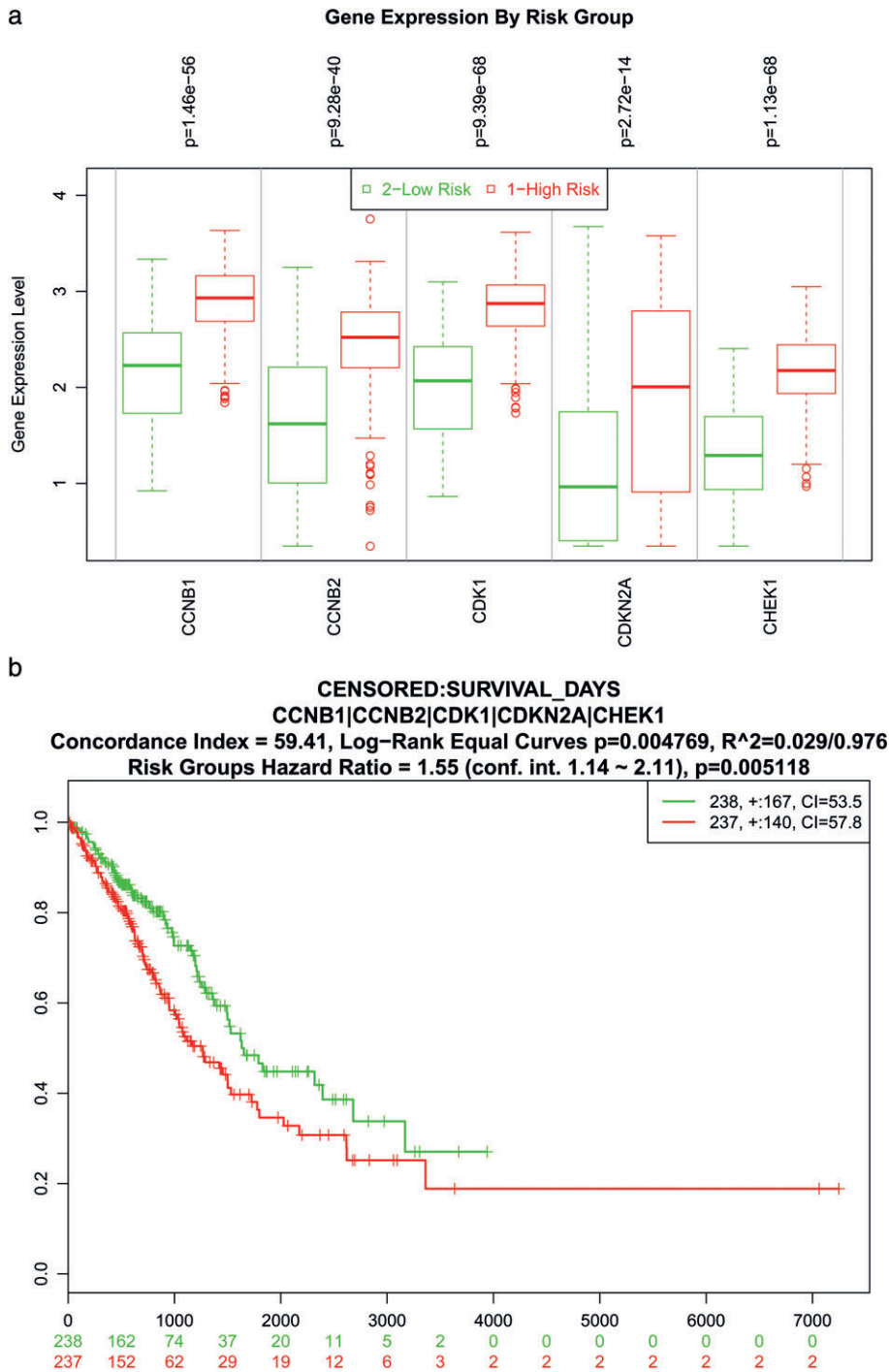
Figure 9 Evaluation of prognosis index in the survival of lung adenocarcinoma patients in The Cancer Genoma Atlas. (**a**) Different expression of the five genes between the high and low-risk groups. (**b**) Kaplan–Meier analysis showed that patients in the high-risk group had a shorter overall time than those in the low-risk.

could potentially provide meaningful assistance in LUAD treatment.

In conclusion, our study highlights critical pathways for the potential treatment of LUAD, most significantly the p53 signaling pathway. Some compounds known for treating LUAD target this pathway, including daunorubicin and mycophenolic acid. Pyrvinium targets the hub gene *CHEK1* directly. However, the effects of several potential LUAD drugs are not well characterized, especially ciclopirox and AG-028671. Future work should concentrate on in vitro and in vivo experiments for these novel compounds to determine if they can be advanced to clinical trials.
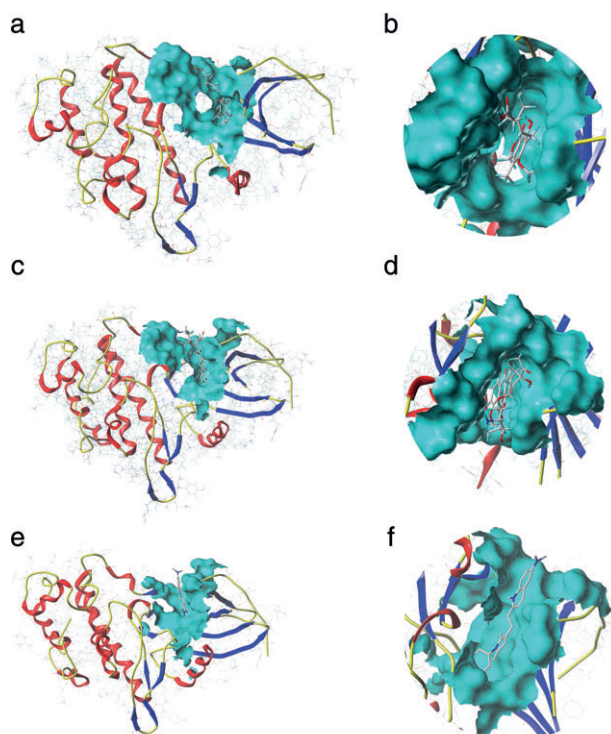
Figure 10 The top three most effective molecules related to *CHEK1* from molecular docking. (**a,b**) Mycophenolic acid with a docking score of 6.9634; (**c,d**) daunorubicin with a docking score of 6.3656; and (**e,f**) pyrvinium with a docking score of 6.2614.

Acknowledgments

Disclosure

No authors report any conflict of interest.

References

1 Basler L, Kroeze SG, Guckenberger M. SBRT for oligoprogressive oncogene addicted NSCLC. *Lung Cancer* 2017; **106**: 50–7.

2 de Langen AJ, Smit EF. Therapeutic approach to treating patients with BRAF-mutant lung cancer: Latest evidence and clinical implications. *Ther Adv Med Oncol* 2017; **9**: 46–58.

3 Saad N, Poudel A, Basnet A, Gajra A. Epidermal growth factor receptor T790M mutation-positive metastatic non-small-cell lung cancer: Focus on osimertinib (AZD9291). *Onco Targets Ther* 2017; **10**: 1757–66.

4 Zhao M, Liu Y, Liu R *et al.* Upregulation of IL-11, an IL-6 family cytokine, promotes tumor progression and correlates with poor prognosis in non-small cell lung cancer. *Cell Physiol Biochem* 2018; **45**: 2213–24.

5 Chen Y, Li C, Pan Y *et al.* The emerging role and promise of long noncoding RNAs in lung cancer treatment. *Cell Physiol Biochem* 2016; **38**: 2194–206.

6 Chen G, Noor A, Kronenberger P, Teugels E, Umelo IA, De Grève J. Synergistic effect of afatinib with su11274 in non-small cell lung cancer cells resistant to gefitinib or erlotinib. *PloS One* 2013; **8**: e59708.

7 Chen G, Umelo IA, Lv S *et al.* miR-146a inhibits cell growth, cell migration and induces apoptosis in non-small cell lung cancer cells. *PloS One* 2013; **8**: e60317.

8 Ghafoor Q, Baijal S, Taniere P, O'Sullivan B, Evans M, Middleton G. Epidermal growth factor receptor (EGFR) kinase inhibitors and non-small cell lung cancer (NSCLC) - Advances in molecular diagnostic techniques to facilitate targeted therapy. *Pathol Oncol Res* 2017. https://doi.org/10.1007/s12253-017-0377-1

9 He RQ, Li XJ, Liang L *et al.* The suppressive role of miR-542-5p in NSCLC: The evidence from clinical data and in vivo validation using a chick chorioallantoic membrane model. *BMC Cancer* 2017; **17**: 655.

10 Masuda C, Yanagisawa M, Yorozu K *et al.* Bevacizumab counteracts VEGF-dependent resistance to erlotinib in an EGFR-mutated NSCLC xenograft model. *Int J Oncol* 2017; **51**: 425–34.

11 Muller IB, de Langen AJ, Giovannetti E, Peters GJ. Anaplastic lymphoma kinase inhibition in metastatic non-small cell lung cancer: Clinical impact of alectinib. *Onco Targets Ther* 2017; **10**: 4535–41.

12 Wang LY, Cui JJ, Guo AX, Yin JY. Clinical efficacy and safety of afatinib in the treatment of non-small-cell lung cancer in Chinese patients. *Onco Targets Ther* 2018; **11**: 529–38.

13 Wang Z, Du T, Dong X, Li Z, Wu G, Zhang R. Autophagy inhibition facilitates erlotinib cytotoxicity in lung cancer cells through modulation of endoplasmic reticulum stress. *Int J Oncol* 2016; **48**: 2558–66.

14 Weng MS, Chang JH, Hung WY, Yang YC, Chien MH. The interplay of reactive oxygen species and the epidermal growth factor receptor in tumor progression and drug resistance. *J Exp Clin Cancer Res* 2018; **37**: 61.

15 Gao L, Zhang LJ, Li SH *et al.* Role of miR-452-5p in the tumorigenesis of prostate cancer: A study based on the Cancer Genome Atl (TCGA), Gene Expression Omnibus (GEO), and bioinformatics analysis. *Pathol Res Pract* 2018; **214**: 732–49.

16 He R, Gao L, Ma J *et al.* The essential role of MTDH in the progression of HCC: A study with immunohistochemistry, TCGA, meta-analysis and in vitro investigation. *Am J Transl Res* 2017; **9**: 1561–79.

17 Li XJ, Pang JS, Li YM *et al.* Clinical value of survivin and its underlying mechanism in ovarian cancer: A bioinformatics study based on GEO and TCGA data mining. *Pathol Res Pract* 2018; **214**: 385–401.

18 Wang X, Li G, Luo Q, Xie J, Gan C. Integrated TCGA analysis implicates lncRNA CTB-193M12.5 as a prognostic factor in lung adenocarcinoma. *Cancer Cell Int* 2018; **18**: 27.

19 Zhang X, Ye ZH, Liang HW *et al.* Down-regulation of miR-146a-5p and its potential targets in hepatocellular carcinoma validated by a TCGA- and GEO-based study. *FEBS Open Bio* 2017; **7**: 504–21.

20 Zhang Y, Li ZY, Hou XX *et al.* Clinical significance and effect of AEG-1 on the proliferation, invasion, and migration of NSCLC: A study based on immunohistochemistry, TCGA, bioinformatics, in vitro and in vivo verification. *Oncotarget* 2017; **8**: 16531–52.

21 Raghavan R, Hyter S, Pathak HB *et al.* Drug discovery using clinical outcome-based Connectivity Mapping: Application to ovarian cancer. *BMC Genomics* 2016; **17**: 811.

22 Shen L, Zhao L, Tang J *et al.* Key genes in stomach adenocarcinoma identified *via* network analysis of RNA-seq data. *Pathol Oncol Res* 2017; **23**: 745–52.

23 Smith I, Greenside PG, Natoli T *et al.* Evaluation of RNAi and CRISPR technologies by large-scale gene expression profiling in the Connectivity Map. *PLoS Biol* 2017; **15**: e2003213.

24 Subramanian A, Narayan R, Corsello SM *et al.* A next generation connectivity map: L1000 platform and the first 1,000,000 profiles. *Cell* 2017; **171**: 1437–52e.17.

25 Wang J, Li M, Wang Y, Liu X. Integrating subpathway analysis to identify candidate agents for hepatocellular carcinoma. *Onco Targets Ther* 2016; **9**: 1221–30.

26 San Lucas FA, Fowler J, Chang K, Kopetz S, Vilar E, Scheet P. Cancer *in silico* drug discovery: A systems biology tool for identifying candidate drugs to target specific molecular tumor subtypes. *Mol Cancer Ther* 2014; **13**: 3230–40.

27 Wang JY, Chen LL, Zhou XH. Identifying prognostic signature in ovarian cancer using DirGenerank. *Oncotarget* 2017; **8**: 46398–413.

28 Gao L, Li SH, Tian YX *et al.* Role of downregulated miR-133a-3p expression in bladder cancer: A bioinformatics study. *Onco Targets Ther* 2017; **10**: 3667–83.

29 Huang C, Yuan N, Wu L *et al.* An integrated analysis for long noncoding RNAs and microRNAs with the mediated competing endogenous RNA network in papillary renal cell carcinoma. *Onco Targets Ther* 2017; **10**: 4037–50.

30 Shen Z, Yu X, Zheng Y *et al.* CDCA5 regulates proliferation in hepatocellular carcinoma and has potential as a negative prognostic marker. *Onco Targets Ther* 2018; **11**: 891–901.

31 Tang Z, Li C, Kang B, Gao G, Li C, Zhang Z. GEPIA: A web server for cancer and normal gene expression profiling and interactive analyses. *Nucleic Acids Res* 2017; **45**: W98–102.

32 He RQ, Yang X, Liang L, Chen G, Ma J. MicroRNA-124-3p expression and its prospective functional pathways in hepatocellular carcinoma: A quantitative polymerase chain reaction, gene expression omnibus and bioinformatics study. *Oncol Lett* 2018; **15**: 5517–32.

33 Lin P, Xiong DD, Dang YW *et al.* The anticipating value of PLK1 for diagnosis, progress and prognosis and its prospective mechanism in gastric cancer: A comprehensive investigation based on high-throughput data and immunohistochemical validation. *Oncotarget* 2017; **8**: 92497–521.

34 Xiong DD, Lv J, Wei KL *et al.* A nine-miRNA signature as a potential diagnostic marker for breast carcinoma: An integrated study of 1,110 cases. *Oncol Rep* 2017; **37**: 3297–304.

35 Zhang Y, He RQ, Dang YW *et al.* Comprehensive analysis of the long noncoding RNA HOXA11-AS gene interaction regulatory network in NSCLC cells. *Cancer Cell Int* 2016; **16**: 89.

36 Li DY, Chen WJ, Luo L *et al.* Prospective lncRNA-miRNA-mRNA regulatory network of long non-coding RNA LINC00968 in non-small cell lung cancer A549 cells: A miRNA microarray and bioinformatics investigation. *Int J Mol Med* 2017; **40**: 1895–906.

37 Liang YY, Huang JC, Tang RX *et al.* Clinical value of miR-198-5p in lung squamous cell carcinoma assessed using microarray and RT-qPCR. *World J Surg Oncol* 2018; **16**: 22.

38 Ren FH, Yang H, He RQ *et al.* Analysis of microarrays of miR-34a and its identification of prospective target gene signature in hepatocellular carcinoma. *BMC Cancer* 2018; **18**: 12.

39 Zhang Y, Dang YW, Wang X *et al.* Comprehensive analysis of long non-coding RNA PVT1 gene interaction regulatory network in hepatocellular carcinoma using gene microarray and bioinformatics. *Am J Transl Res* 2017; **9**: 3904–17.

40 Jaravine V, Mösch A, Raffegerst S, Schendel DJ, Frishman D. Expitope 2.0: A tool to assess immunotherapeutic antigens for their potential cross-reactivity against naturally expressed proteins in human tissues. *BMC Cancer* 2017; **17**: 892.

41 Liu W, Ye H, Liu YF *et al.* Transcriptome-derived stromal and immune scores infer clinical outcomes of patients with cancer. *Oncol Lett* 2018; **15**: 4351–7.

42 Myint KZ, Kongpracha P, Rattanasinganchan P *et al.* Gadd45beta silencing impaired viability and metastatic phenotypes in cholangiocarcinoma cells by modulating the EMT pathway. *Oncol Lett* 2018; **15**: 3031–41.

43 Negrini M. Change of title: Microarrays becomes High-Throughput. *High Throughput* 2017; **6**: 10.

44 Thul PJ, Åkesson L, Wiking M *et al.* A subcellular map of the human proteome. *Science* 2017; **356**: eaal3321.

45 Uhlén M, Fagerberg L, Hallström BM *et al*. Proteomics. Tissue-based map of the human proteome. *Science* 2015; **347**: 1260419.

46 Uhlen M, Zhang C, Lee S *et al*. A pathology atlas of the human cancer transcriptome. *Science* 2017; **357**: pii: eaan2507.

47 Aguirre-Gamboa R, Gomez-Rueda H, Martínez-Ledesma E *et al*. SurvExpress: An online biomarker validation tool and database for cancer gene expression data using survival analysis. *PloS One* 2013; **8**: e74250.

48 Gao J, Zhao S, Halstensen TS. Increased interleukin-6 expression is associated with poor prognosis and acquired cisplatin resistance in head and neck squamous cell carcinoma. *Oncol Rep* 2016; **35**: 3265–74.

49 Gao X, Dai M, Li Q, Wang Z, Lu Y, Song Z. HMGA2 regulates lung cancer proliferation and metastasis. *Thorac Cancer* 2017; **8**: 501–10.

50 Kunicka T, Prochazka P, Krus I *et al*. Molecular profile of 5-fluorouracil pathway genes in colorectal carcinoma. *BMC Cancer* 2016; **16**: 795.

51 Lee YC, Huang CC, Lin DY, Chang WC, Lee KH. Overexpression of centromere protein K (CENPK) in ovarian cancer is correlated with poor patient survival and associated with predictive and prognostic relevance. *PeerJ* 2015; **3**: e1386.

52 Namani A, Matiur Rahaman M, Chen M, Tang X. Gene-expression signature regulated by the KEAP1-NRF2-CUL3 axis is associated with a poor prognosis in head and neck squamous cell cancer. *BMC Cancer* 2018; **18**: 46.

53 Shan YS, Hsu HP, Lai MD, Yen MC, Luo YP, Chen YL. Increased expression of argininosuccinate synthetase protein predicts poor prognosis in human gastric cancer. *Oncol Rep* 2015; **33**: 49–57.

54 Homer RW, Swanson J, Jilek RJ, Hurst T, Clark RD. SYBYL line notation (SLN): a single notation to represent chemical structures, queries, reactions, and virtual libraries. *J Chem Inf Model* 2008; **48**: 2294–307.

55 Koelmel JP, Ulmer CZ, Jones CM, Yost RA, Bowden JA. Common cases of improper lipid annotation using high-resolution tandem mass spectrometry data and corresponding limitations in biological interpretation. *Biochim Biophys Acta* 1862; **2017**: 766–70. (Published erratum appears in *Biochim Biophys Acta* 2017; **1862**: 1024).

56 Preston S, Jiao Y, Baell JB *et al*. Screening of the 'Open Scaffolds' collection from Compounds Australia identifies a new chemical entity with anthelmintic activities against different developmental stages of the barber's pole worm and other parasitic nematodes. *Int J Parasitol Drugs Drug Resist* 2017; **7**: 286–94.

57 Du Y, Hao X, Liu X. Low expression of long noncoding RNA CDKN2B-AS1 in patients with idiopathic pulmonary fibrosis predicts lung cancer by regulating the p53-signaling pathway. *Oncol Lett* 2018; **15**: 4912–8.

58 Feng HM, Zhao Y, Zhang JP *et al*. Expression and potential mechanism of metabolism-related genes and CRLS1 in non-small cell lung cancer. *Oncol Lett* 2018; **15**: 2661–8.

59 Gao W, Liu L, Xu J *et al*. A systematic analysis of predicted MiR-31-targets identifies a diagnostic and prognostic signature for lung cancer. *Biomed Pharmacother* 2014; **68**: 419–27.

60 Guo CL, Wang LJ, Zhao Y *et al*. A novel bromophenol derivative BOS-102 induces cell cycle arrest and apoptosis in human A549 lung cancer cells via ROS-mediated PI3K/Akt and the MAPK signaling pathway. *Mar Drugs* 2018; **16**: pii: E43.

61 Lei L, Zeng Q, Lu J *et al*. MALAT1 participates in ultraviolet B-induced photo-aging via regulation of the ERK/MAPK signaling pathway. *Mol Med Rep* 2017; **15**: 3977–82.

62 Lin S, Lv J, Peng P *et al*. Bufadienolides induce p53-mediated apoptosis in esophageal squamous cell carcinoma cells in vitro and in vivo. *Oncol Lett* 2018; **15**: 1566–72.

63 Liu J, Yang XY, Shi WJ. Identifying differentially expressed genes and pathways in two types of non-small cell lung cancer: Adenocarcinoma and squamous cell carcinoma. *Genet Mol Res* 2014; **13**: 95–102.

64 Liu Y, Wang P, Li S, Yin L, Shen H, Liu R. Interaction of key pathways in sorafenib-treated hepatocellular carcinoma based on a PCR-array. *Int J Clin Exp Pathol* 2015; **8**: 3027–35.

65 Stankevicius V, Vasauskas G, Bulotiene D *et al*. Gene and miRNA expression signature of Lewis lung carcinoma LLC1 cells in extracellular matrix enriched microenvironment. *BMC Cancer* 2016; **16**: 789.

66 Yuan S, Qiao T, Li X *et al*. Toll-like receptor 9 activation by CpG oligodeoxynucleotide 7909 enhances the radiosensitivity of A549 lung cancer cells via the p53 signaling pathway. *Oncol Lett* 2018; **15**: 5271–9.

67 Zhang HY, Yang W, Lu JB. Knockdown of GluA2 induces apoptosis in non-small-cell lung cancer A549 cells through the p53 signaling pathway. *Oncol Lett* 2017; **14**: 1005–10.

68 Zhang Y, Dong H, Zhang J, Zhang L. Inhibitory effect of hyperoside isolated from *Zanthoxylum bungeanum* leaves on SW620 human colorectal cancer cells via induction of the p53 signaling pathway and apoptosis. *Mol Med Rep* 2017; **16**: 1125–32.

69 Balasubramaniam S, Redon CE, Peer CJ *et al*. Phase I trial of belinostat with cisplatin and etoposide in advanced solid tumors, with a focus on neuroendocrine and small cell cancers of the lung. *Anticancer Drugs* 2018; **29**: 457–65.

70 Dai W, Jiang Y, Chen K *et al*. Effect of etoposide-induced alteration of the Mdm2-Rb signaling pathway on cellular senescence in A549 lung adenocarcinoma cells. *Oncol Lett* 2017; **14**: 3935–40.

71 Morabito A, Daniele G, Costanzo R *et al*. A multicenter, randomized, phase 3 trial comparing fixed dose versus toxicity-adjusted dose of cisplatin + etoposide in extensive small-cell lung cancer (SCLC) patients: The Small-cell-lung

Cancer Toxicity Adjusted Dosing (STAD-1) Trial. *Lung Cancer* 2017; **108**: 15–21.

72 Bai Y, Wu HW, Ma X, Liu Y, Zhang YH. Relationship between *UGT1A1*6/*28* gene polymorphisms and the efficacy and toxicity of irinotecan-based chemotherapy. *Onco Targets Ther* 2017; **10**: 3071–81.

73 Fukuda M, Okumura M, Iwakiri T *et al*. Relationship between *UGT1A1*27* and *UGT1A1*7* polymorphisms and irinotecan-related toxicities in patients with lung cancer. *Thorac Cancer* 2018; **9**: 51–8.

74 Kondo R, Watanabe S, Shoji S *et al*. A phase II study of irinotecan for patients with previously treated small-cell lung cancer. *Oncology* 2018; **94**: 223–32.

75 Misumi Y, Okamoto H, Sasaki J *et al*. Phase I/II study of induction chemotherapy using carboplatin plus irinotecan and sequential thoracic radiotherapy (TRT) for elderly patients with limited-disease small-cell lung cancer (LD-SCLC): TORG 0604. *BMC Cancer* 2017; **17**: 377.

76 Xu RH, Muro K, Morita S *et al*. Modified XELIRI (capecitabine plus irinotecan) versus FOLFIRI (leucovorin, fluorouracil, and irinotecan), both either with or without bevacizumab, as second-line therapy for metastatic colorectal cancer (AXEPT): A multicentre, open-label, randomised, non-inferiority, phase 3 trial. *Lancet Oncol* 2018; **9**: 660–71.

77 de Freitas Silva M, Coelho LF, Guirelli IM *et al*. Synthetic resveratrol-curcumin hybrid derivative inhibits mitosis progression in estrogen positive MCF-7 breast cancer cells. *Toxicol In Vitro* 2018; **50**: 75–85.

78 Feng Y, Zhou J, Jiang Y. Resveratrol in lung cancer - A systematic review. *J BUON* 2016; **21**: 950–3.

79 Takashina M, Inoue S, Tomihara K *et al*. Different effect of resveratrol to induction of apoptosis depending on the type of human cancer cells. *Int J Oncol* 2017; **50**: 787–97.

80 Bains OS, Szeitz A, Lubieniecka JM *et al*. A correlation between cytotoxicity and reductase-mediated metabolism in cell lines treated with doxorubicin and daunorubicin. *J Pharmacol Exp Ther* 2013; **347**: 375–87.

81 Cavarretta E, Mastroiacovo G, Lupieri A, Frati G, Peruzzi M. The positive effects of exercise in chemotherapy-related cardiomyopathy. *Adv Exp Med Biol* 2017; **1000**: 103–29 (Published erratum appears in (Published erratum appears in *Adv Exp Med Biol* 2017; **1000**: E1).

82 de Oliveira VA, da Motta LL, De Bastiani MA *et al*. In vitro evaluation of antitumoral efficacy of catalase in combination with traditional chemotherapeutic drugs against human lung adenocarcinoma cells. *Tumour Biol* 2016; **37**: 10775–84.

83 Momtazi-Borojeni AA, Abdollahi E, Ghasemi F, Caraglia M, Sahebkar A. The novel role of pyrvinium in cancer therapy. *J Cell Physiol* 2018; **233**: 2871–81.

84 Aziz SI, Khattak MA, Usmani Z, Ladipeerla N, Pittman K. Metyrapone: A management option for ectopic ACTH syndrome in small cell lung cancer treated with intravenous etoposide. *BMJ Case Rep* 2011. https://doi.org/10.1136/bcr.04.2010.2917

85 Chokshi S, Hochster HS. Single-agent therapies after standard combination regimens. *Cancer J* 2016; **22**: 205–10.

86 Scagliotti G, Nishio M, Satouchi M *et al*. A phase 2 randomized study of TAS-102 versus topotecan or amrubicin in patients requiring second-line chemotherapy for small cell lung cancer refractory or sensitive to frontline platinum-based chemotherapy. *Lung Cancer* 2016; **100**: 20–3.

87 Domhan S, Schwager C, Wei Q *et al*. Deciphering the systems biology of mTOR inhibition by integrative transcriptome analysis. *Curr Pharm Des* 2014; **20**: 88–100.

88 Spain L, Diem S, Larkin J. Management of toxicities of immune checkpoint inhibitors. *Cancer Treat Rev* 2016; **44**: 51–60.

89 Mihailidou C, Papakotoulas P, Papavassiliou AG, Karamouzis MV. Superior efficacy of the antifungal agent ciclopirox olamine over gemcitabine in pancreatic cancer models. *Oncotarget* 2018; **9**: 10360–74.

90 Shen T, Shang C, Zhou H *et al*. Ciclopirox inhibits cancer cell proliferation by suppression of Cdc25A. *Genes Cancer* 2017; **8**: 505–16.

91 Yuan B, Ji W, Xia H, Li J. Combined analysis of gene expression and genome binding profiles identified potential therapeutic targets of ciclopirox in Ewing sarcoma. *Mol Med Rep* 2018; **17**: 4291–8.

Supporting Information

Additional Supporting Informationmay be found in the online version of this article at the publisher's website:

Figure S1 Chemical structures of the top 10 significant molecules. (**a**) etoposide; (**b**) irinotecan; (**c**) camptothecin; (**d**) pyrvinium; (**e**) metyrapone; (**f**) trifluridine; (**g**) mycophenolic acid; (**h**) resveratrol; (**i**) AG-028671; and (**j**) daunorubicin.

Figure S2 Differentially expressed genes (DEGs) between lung adenocarcinoma and normal tissues. (**a**) The DEG positions based on GRCh38.p2 (NCBI); and (**b**) a volcano plot displaying the DEGs.

Figure S3 Small molecular drugs and their predicted pathways in lung adenocarcinoma. The yellow nodes represent drugs, and the blue nodes represent pathway.

Figure S4 Protein–protein interactions of five overlapping pathways. (**a**) Pathway in cancer; and (**b**) MAPK, (**c**) p53, (**d**) chemokine, and (**e**) Fc epsilon RI signaling pathways.

Figure S5 The messenger RNA expression level of five hub genes in p53 signaling pathway: (**a**) *CCNB1*, (**b**) *CCMB2*, (**c**) *CDK1*, (**d**) *CDKN2A*, and (**e**) *CHEK1*.

Table S1 Significant Kyoto Encyclopedia of Genes and Genomes (KEGG) pathways of differentially expressed genes in lung adenocarcinoma.

Table S2 Molecular docking results for *CHEK1*.